Journal of Catalysis **194,** 140–145 (2000)
doi:10.1006/jcat.2000.2923, available online at http://www.idealibrary.com on IDEAL®

In Situ XRD Investigations of Heteropolyacid Catalysts in the Methacrolein to Methacrylic Acid Oxidation Reaction: Structural Changes during the Activation/Deactivation Process

L. Marosi,[1] G. Cox, A. Tenten, and H. Hibst

BASF AG, 67056 Ludwigshafen, Germany

Received February 23, 2000; revised May 4, 2000; accepted May 5, 2000

The structural changes of $CsH_2PMo_{12}O_{40}$ Keggin-type heteropolyacid under the conditions of the methacrolein to methacrylic acid oxidation have been studied by *in situ* X-ray powder diffraction with simultaneous measurement of the activity and selectivity of the catalysts. The results of the present studies show that under the operating conditions migration of Mo atoms from the Keggin unit into the intracrystalline pore system takes place. The working catalyst is characterized by the presence of Mo in the intracrystalline pore system of the crystal lattice. However, the migration of Mo atoms has been found to be a progressive process which, with increasing time on stream, finally results in the destruction of the Keggin units. The observed activity decline is correlated with the decomposition of the heteropolyacid under formation of catalytically less active MoO_3.

Key Words: **heteropolyacids; methacrolein; methacrylic acid; *in situ* XRD; structure–activity relationships; promoter effect.**

INTRODUCTION

Heteropolyacid (HPA) catalysts are enjoying great interest in many important industrial homogeneous and heterogeneous catalytic processes (1, 2). Due to their bifunctional character HPA catalysts are appropriate catalysts for both acid-catalyzed and redox reactions. The combination of strong Brønsted acidity with high redox activity renders HPA as suitable catalysts for many oxidation reactions. For example, HPA of the type $Cs_xH_{3+y-x}PV_yMo_{12-x}O_{40}$ ($x = 0$–2; $y = 1$, 2) are used as catalysts for the oxidation of methacrolein (MA) and of isobutyric acid (IBA) to methacrylic acid (MAA) on an industrial scale (3, 4). A drawback of these catalysts is their relatively short lifetime under the operating conditions of the industrial process (5, 6).

Therefore, numerous studies have been carried out on the thermal stability of different HPA and HPA salts (7–10) and on the role of the different promoters contained in industrial catalysts.

The role of vanadium on activity, selectivity, and stability has been studied by several authors (11–14). By characterizing used catalysts by a set of physicochemical techniques Cadot *et al.* showed that use of HPA in IBA oxidation leads to release of vanadium atoms from the initial Keggin structure (14). It was concluded that under the conditions of the reaction vanadium is present as VO_2^+ cation and stabilizes the cubic Keggin structure.

The structure of $H_4PVMo_{11}O_{40}$ under the reaction conditions of the IBA to MAA oxidation has been studied recently by means of the *in situ* XRD technique by Ilkenhans *et al.* (15). The authors concluded that under the conditions of the reaction VO^{2+} cations are formed. The cubic vanadyl salt is supposed to be an active phase in IBA to MAA oxidation.

The effect of cesium salt formation on selectivity and thermal stability in the oxidation of MA to MAA has been studied by Misono *et al.* (16) and Deußer *et al.* (17) and was also described in some patent applications (18). It was found that Cs has a beneficial effect on selectivity as well as on thermal stability of HPA catalysts.

Despite improvements achieved by these modifications the lifetime of MAA catalysts remains still unsatisfactory. The mechanism of the deactivation process and the corresponding structural changes of the catalyst are not well understood yet.

Because knowledge of the structure is an important step toward understanding the mechanism of the reaction and the thermal stability, the determination of structures present in working catalysts and of structural changes during the catalyst aging process is of great interest for further improvement of catalytic properties. The aim of this study is to elucidate the structure of HPA catalysts under the conditions of the MA to MAA oxidation and of the structural changes with temperature and increasing time on stream in order to obtain better insight into the reaction mechanism and into the nature of the catalyst deactivation process.

[1] To whom correspondence should be addressed. Fax: 0049 621 626475. E-mail: Marosi@t-online.de.

0021-9517/00 $35.00

METHODS

1. Sample Preparation

Samples of $CsH_2PMo_{12}O_{40}$ (abbreviated as CsHPMo12) were prepared according to a method previously described (17). Starting materials for the preparation were ammonium molybdate, phosphoric acid (76%), cesium nitrate, and nitric acid (65%). According to the desired stoichiometry phosphoric acid was added with an excess of 5%.

The raw materials were dissolved in water in the sequence given above. Nitric acid was added in such an amount that the pH of the resulting solution was between 1.5 and 1.8. Precipitation took place during addition of nitric acid. The suspension was evaporated to dryness. The resulting solid was ground and characterized by XRD. Two crystalline structures were present, NH_4NO_3 and a structure of the type $(NH_4)_3PMo_{12}O_{40} \cdot 4H_2O$. The product was tableted to 5- $\times$ 5-mm cylinders. The tablets were calcined. The temperature program for calcination consisted of a 24-h heating period up to 653 K at constant rate. The temperature of 653 ± 2 K was held constant for a period of 5 h and then the product was cooled in a stream of dry air. The cylinders were crushed and sieved to the mesh size of 0.2–0.4 mm. The product was stored tightly sealed under dry conditions.

2. Sample Characterization

The catalyst was characterized by chemical analysis, by means of XRD analysis, BET surface area, and porosimetry measurements by Hg penetration. After the calcination procedure the XRD diagram showed a pure monophasic compound having the cubic Keggin structure. The BET surface area was 5.4 m^2/g and the porosity value 0.24 ml/g. The lattice constants for the fresh and used catalyst were 1.1749 nm and 1.1834 nm, respectively. The lattice constant for the fresh catalyst is in good agreement with literature data (19).

3. In situ XRD Setup

The flow diagram of the experimental setup used for simultaneous XRD and catalytic measurements is schematically represented in Fig. 1. The apparatus consists of three parts:

(1) the dosing unit for the gaseous and liquid reactants,

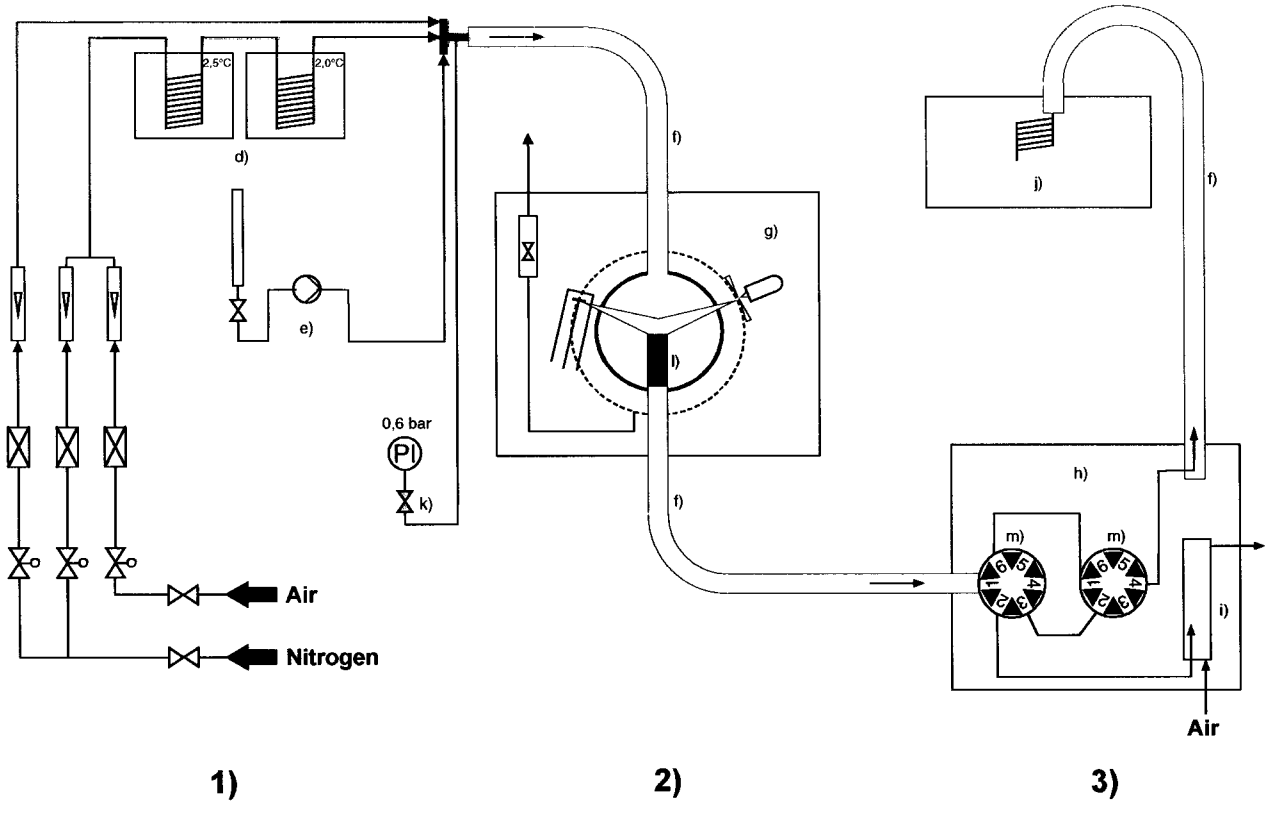

FIG. 1. Flow diagram of the *in situ* XRD experimental unit: (a) reducing valves, (b) electronic gas flow controller, (c) rotameter, (d) saturator, (e) nitrogen floating unit, (f) heated pipe, (g) X-ray diffractometer, (h) warming cupboard, (i) combustion reactor, (j) gas chromatograph, (k) pressure relief valve, (l) reactor, and (m) multiway valves.

(2) the XRD diffractometer equipped with the *in situ* reaction chamber, and

(3) the online GC analytical part.

Dosing of MA was carried out by saturation of a nitrogen flow in liquid MA at 275 K. Dosing of water was performed by use of a microprecision pump. The gaseous feed consisting of MA, air, N_2, and H_2O was preheated to 473 K and introduced directly into the *in situ* chamber. The *in situ* XRD chamber was a commercially available Paar high-temperature chamber which was modified with a special sample holder having a 5-ml catalyst bed volume and a modified heating system. The thermocouple was embedded in the catalyst bed. The temperature was controlled within ± 2 K. In order to prevent polymerization of the reaction products the outlet gas temperature was kept to 533 K and analyzed online using a Perkin Elmer gas chromatograph equipped with a thermal conductivity detector and a capillary column. Exhaust gases from the reactor and from the GC were introduced onto a total combustion reactor and converted into CO_2 on a platinum catalyst.

X-ray diffraction (XRD) patterns were obtained by a Siemens D-5000 θ/θ diffractometer using Cu Kα radiation.

4. Reaction Conditions

The standard feed composition was 1.17 g of MA, 1.02 g of H_2O, 3.51 of air, and 2.821 of N_2/5 g of catalyst, h.

The catalytic oxidation was performed between temperatures from 593 K to 633 K. The catalyst was granulated into particles from 0.2 to 0.4 mm in size. Before catalytic measurement the catalyst was preconditioned at 473 K for 1 h under air and then for 2 h under the flow reaction gas. The temperature was then slowly increased to the desired reaction temperature.

RESULTS AND DISCUSSION

Oxidation of MA over CsHPMo12

In the temperature range between 593 K and 613 K changes in XRD were only small. In addition to this the observed changes in intensity were of temporary nature and reversible with time. Nevertheless, the fluctuations in intensity were significant and in their tendency very similar to those observed at higher temperatures.

At 625 K characteristic changes in XRD diagrams were observed revealing major differences in both relative integrated intensities I/I_0 and peak positions. Figure 2 shows the examples of XRD patterns obtained under standard reaction conditions. The relative intensities I/I_0 show major differences compared with the fresh sample (Fig. 2a) and vary slightly with time between those shown in Figs. 2b–2d. Although changes in relative intensity affect all the observed diffraction lines the alterations in intensity are especially conspicuous when inspecting the diffraction lines in the 2θ range between 18 and 26°.

With increasing time on stream the changes in intensity become more and more pronounced and, moreover, increasing formation of MoO_3 can be observed (Fig. 3).

In order to identify the structural alterations responsible for the observed changes in XRD patterns, intensity

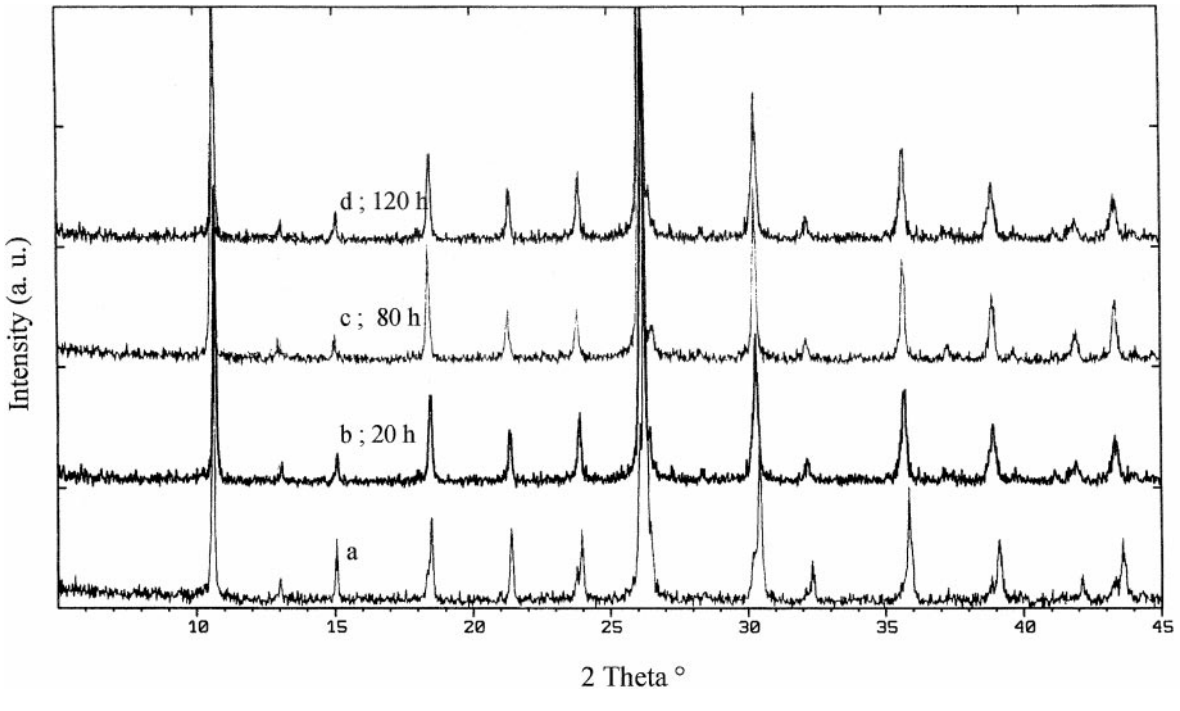

FIG. 2. *In situ* diffraction patterns at 625 K with increasing time on stream, 0–120 h, (a) without MA supply, and (b)–(d) MA supply on.

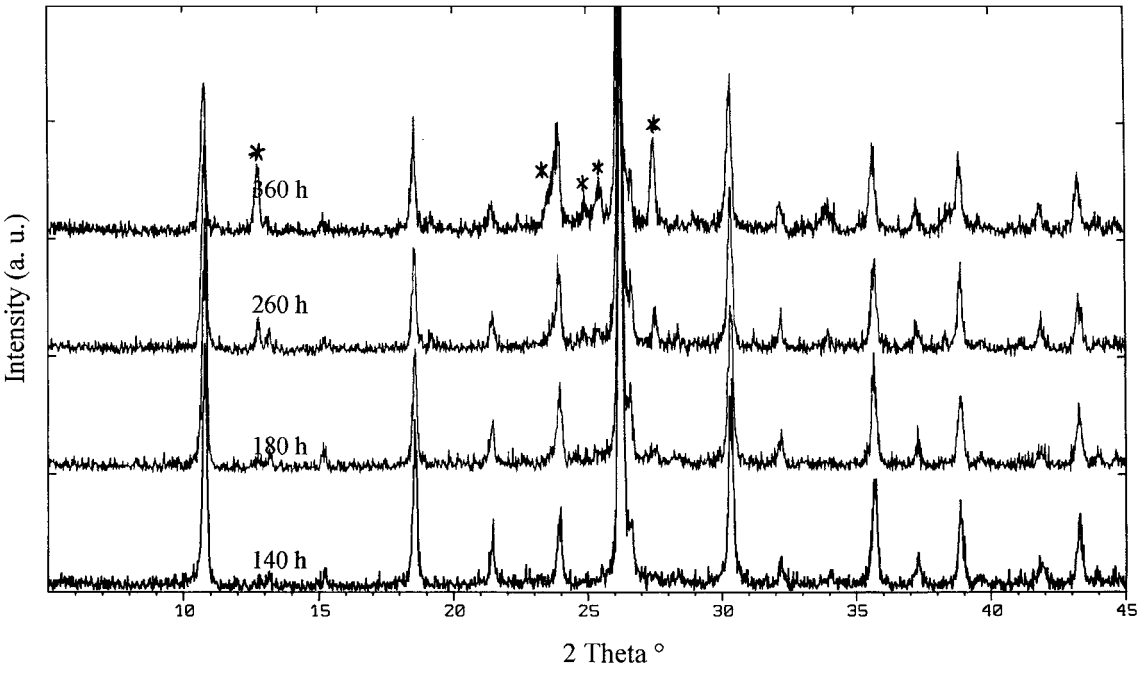

FIG. 3. *In situ* diffraction diagrams at 625 K with increasing time on stream, 120–360 h. Peaks corresponding to MoO_3 are marked.

calculations have been carried out using several structure models by varying fractional coordinates of Mo and O atoms in the Keggin unit by varying Cs fractional coordinates in the intracrystalline pore system and by moving Mo atoms from the Keggin unit into the pores. The modeling of XRD patterns showed that the measured changes in relative intensities can only be simulated in a satisfactory way by moving Mo atoms from the Keggin unit into the intracrystalline pore system.

Following the model calculation Rietveld refinements of the atomic coordinates derived from the best-fitting structure model have been performed. The result of Rietveld profile fitting is given in Fig. 4. It shows good agreement between the measured and calculated intensities ($S = R_{WP}/R_{EXP} = 1.29$; $R_{Bragg} = 8.06\%$). Most of the resulting differences between measured and calculated intensities are due to a nonsystematic broadening of some of the diffraction lines. A similar effect of peak broadening has been observed for $(VO)_2P_2O_7$ catalysts in the butane oxidation reaction (23). The results of the analysis of the observed peak broadening and the structural details of the situation of the Mo(2) atoms in the pores of the active HPA salt will be published in a separate paper.

The resulting atomic coordinates are presented in Table 1. The lowering of the occupancy factors of the Mo(1)—and O(1–3)—atoms from 12 to the calculated

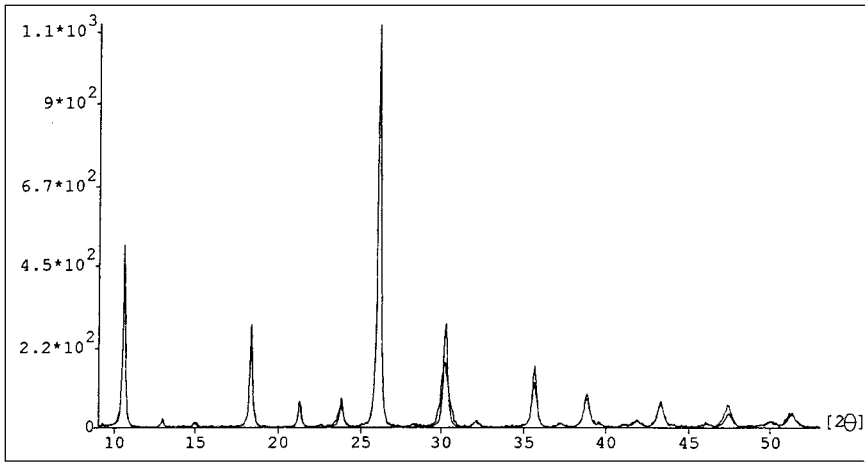

FIG. 4. Rietveld refinement plot of a used catalyst, observed (continuous line) and calculated (dotted line) XRD pattern. Goodness of fit $S = R_{WP}/R_{EXP} = 1.29$; $R_{Bragg} = 0.08$.

TABLE 1

Fractional Atomic Coordinates

	x	*y*	*z*	*k*
Mo(1)	0.4663	0.4663	0.2561	11.4249
Mo(2)	0.7487	0.7266	0.3362	1.3249
Mo(2)′	0.2500	0.7500	0.7500	0.3600
O(1)	0.6582	0.6582	0.0112	11.4547
O(2)	0.0639	0.0639	0.7736	11.4203
O(3)	0.1301	0.1301	0.5424	11.8658
O(4)	0.3283	0.3283	0.3283	4.0
P	0.75	0.75	0.75	1.0
Cs	0.25	0.75	0.75	1.0

Note. Mo(2) and Mo(2)′ represent Mo atoms in the intracrystalline pore system of the HPA; k = stoichiometric occupancy factor.

values between 11 and 12 is in conformity with recent results of IR—and Raman—spectroscopy. It has been shown (24) that under the conditions of the reaction lacunary PMo_{12-x} Keggin units are formed which in the presence of moisture undergo a reversible restructuring process. The working state of the catalyst is characterized by the presence of defects in the anionic structure. The Mo(2) atoms are located in the interstices between the polyanions but their atomic fractional coordinates differ significantly from the ideal positions for alkali metal ions in cubic HPA salts. The Mo(2) atoms are closer to the heteropolyanions as cations occupying the exact crystallographic positions and are probably bound to oxygen atoms of the polyanion.

In view of these results it is interesting to consider the changes of lattice constant as a function of run time: a_o increased continuously as the changes in intensity became more and more pronounced. This phenomenon may be related to the ionic radii of the Mo oxospecies formed by the catalytic interaction. In $Na_2(VO)(SiW_{12}O_{40} \cdot 13H_2O$ (14) the vanadium atoms are hexacoordinated as $VO(H_2O)_5^{2+}$ cations and are located in the interstices between polyanions. Depending on the experimental conditions VO^{2+} ions can be dehydrated (bound to the heteropolyanion) or in the hydrated form. As the ionic radii of such oxospecies are expected to be larger than the ionic radii of Cs atoms, the large increase of the lattice constant from 1.1749 nm to 1.1843 nm is a plausible result of the molybdenum migration process.

Corresponding to the observed structural changes, the activity and selectivity of the catalyst follow those of Mo migration and MoO_3 formation:

Within the first 120 h on stream conversion and selectivity increased from 63.6% to 68.4% and from 56% to 58.5%, respectively (Fig. 5). Apparently, the formation of cationic Mo species exerts a beneficial effect on both activity and selectivity of the catalyst.

Between 120 and 320 h time on stream activity falls to 63% whereas selectivity diminishes from 58.5% to 54%. Figure 3 shows that the observed decrease in activity and selectivity is correlated with growing formation of MoO_3.

These results clearly show that the formation of cationic species as previously reported in the literature for HPVMo11 is not restricted to VO^{2+} cations. During the catalytic reaction a similar migration of molybdenum atoms from the Keggin unit into the pores of the crystal lattice takes place and these atoms are probably present as cationic Mo oxospecies.

Moreover, the migration of Mo oxospecies has been found to be a progressive process which, depending on reaction temperature and time on stream, necessarily leads to

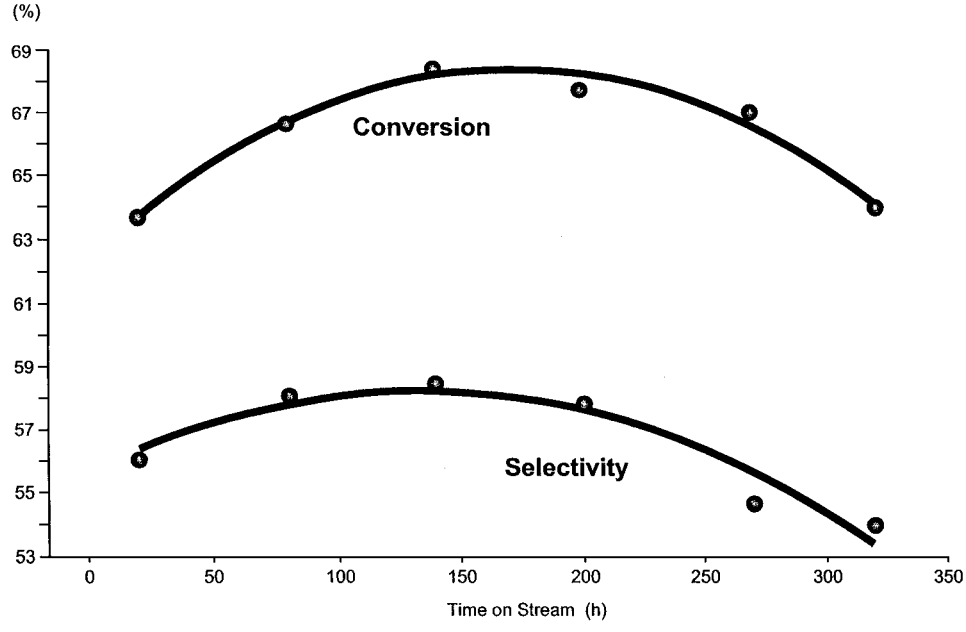

FIG. 5. Activity and selectivity vs time at 625 K.

the destruction of the crystal structure under formation of catalytically less active MoO_3 and this process seems to be responsible for the long-term deactivation of the catalyst.

Effects of Oxygen and Steam in the Gas Phase

Variation of H_2O. The presence of steam had a remarkable effect both on activity and on selectivity. The activity and selectivity of the catalyst drop dramatically with decreasing water content in the feed but without any changes in crystal structure. When water was turned off completely (steam was replaced by nitrogen during the measurement period) the activity decreased from 65% to 37% conversion whereas selectivity diminished from 57% to 39%. When the water was reintroduced into the reaction the catalyst's activity and selectivity increased again and reached their original values after about 6 h on stream. Water consequently has no effect on the catalyst bulk structure. The role of water is probably restricted to a surface effect or to adsorption/desorption phenomena (20–22).

Variation of air. The variation of air from an air to MA ratio of 6 : 1 to 2 : 1 had no effect on the activity or selectivity values. A further decrease in air to air to MA < 1 : 1 leads to decreasing activity values. When the supply of air was stopped completely the reaction continued for a prolonged period of time. The selectivity to MAA remained rather constant although the rate decreased significantly.

A similar effect has been reported in the literature by Konishi *et al*. for the same reaction (22). After the standard reaction conditions were restored the activity and selectivity reached their original values again. The crystal structure of the catalyst remained unchanged during these operations even in a pure MA atmosphere.

CONCLUSIONS

We have shown that under the reaction conditions migration of Mo oxospecies from the Keggin unit into the intracrystalline pore system of the crystal lattice takes place and this process has two kinds of roles affecting the activity, the selectivity, and the lifetime of the catalyst.

On one hand the presence of cationic Mo oxospecies in the intracrystalline pore system represents the active state of the working catalyst and exerts a beneficial effect on both activity and selectivity.

On the other hand the progressive migration of Mo atoms leads with increasing time on stream to the destruction of the HPA structure under formation of catalytically less active MoO_3. This process appears to be responsible for the long-term catalyst deactivation.

The former role predominates at low reaction temperatures; the latter gains an increasing role at higher reaction temperatures and with increasing time on stream.

However, our investigations show that the second effect is not exclusively due to a purely thermal stress. The decomposition of the catalyst seems to be essentially bound up with the nature of the redox catalytic process. Without catalytic interaction with MA the Keggin structure is thermally stable up to temperatures of 693 K (8). Longer catalyst lifetime can therefore be achieved either by a proper stabilization of the Keggin structure or by the development of more active catalysts, working at lower reaction temperatures. At temperatures lower than 593 K the migration of Mo atoms has been found to be a very slow process and the formation of MoO_3 is nearly negligible.

Attempts to develop more active catalysts by structural promoters may be a promising way toward the development of more efficient catalysts for the MA to MAA oxidation reaction.

ACKNOWLEDGMENTS

Financial support by the Bundesministerium für Bildung, Wissenschaft, Forschung and Technologie and by the BASF AG is gratefully acknowledged.

REFERENCES

1. Misono, M., *Catal. Rev. Sci. Eng.* **29**, 269–321 (1987).
2. Mizuno, N., and Misono, M., *Chem. Rev.* **98**, 199–217 (1998).
3. Japan Patent 1975-23013 (Mitsubishi Rayon).
4. Akimoto, M., Shirna, K., Ikeda, H., and Echigoya, E., *J. Catal.* **86**, 173 (1984).
5. Haeberle, T., and Emig, G., *Chem. Eng. Technol.* **11**, 392–402 (1988).
6. Popova, G. Ya., and Andrushkevich, T. V., *Kinet. Catal.* **35**, 120–123 (1994).
7. Rabia, M. C., Hervé, G., Launay, S., Fournier, M., and Feumi-Jantou, C., *J. Mater. Chem.* **2**(9), 971–978 (1992).
8. Albonetti, S., Cavani, F., Trifirò, F., Gazzano, M., Koutyrev, M., Aissi, F. C., Aboukais, A., and Guelton, M., *J. Catal.* **146**, 491–502 (1994).
9. Rocchiccioli-Deltcheff, C., Aouissi, A., Bettahar, M. M., Launay, S., and Fournier, M., *J. Catal.* **164**, 16–27 (1996).
10. Bielanski, A., Malecka, A., and Kubelkova, K., *J. Chem. Soc., Faraday Trans., 1* **85**(9), 2847–2856 (1989).
11. Bergier, T., Brückmann, K., and Haber, J., *Recl. Trav. Chim. Pays-Bas* **113**, 475–480 (1994).
12. Marchal-Roch, C., Bayer, R., Moisan, J. F., Tézé, A., and Harvé, G., *Top. Catal.* **3**, 407–419 (1996).
13. Cesarini, D., Centi, G., Jíru, P., Lena, V., and Tvaružková, Z., *J. Catal.* **143**, 325–344 (1993).
14. Cadot, E., Marchal, C., Fournier, M., Tézé, A., and Hervé, G., *in* "Polyoxometalates" (M. T. Pope and A. Müller, Eds.), pp. 315–326. Kluwer Academic, Dordrecht, 1994.
15. Ilkenhans, Th., Herzog, B., Brown, Th., and Schlögl, R., *J. Catal.* **153**, 275–292 (1995).
16. Mizuno, N., Watanabe, T., and Misono, M., *Bull. Chem. Soc. Jpn.* **64**, 243 (1991).
17. Deußer, L. M., Gaube, J. W., Martin, F. G., and Hibst, H., *Stud. Surf. Sci. Catal.* **101**, 981–990 (1996).
18. Japan Patent JP 04063139 A2, 1992 (Sumitomo Kagaku Kogyo K. K.).
19. McGarway, G. B., and Moffat, J. B., *J. Catal.* **130**, 483–497 (1991).
20. Okuhara, T., Hashimoto, T., Hibi, T., and Misono, M., *J. Catal.* **93**, 224–230 (1985).
21. Ernst, V., Barbaux, Y., and Courtine, P., *Catal. Today* **1**, 167–180 (1987).
22. Konishi, Y., Sakata, K., Misono, M., and Yoneda, Y., *J. Catal.* **77**, 169–179 (1982).
23. Nguyen, P. T., and Sleight, A. W., *J. Solid State Chem.* **122**, 259–265 (1996).
24. Ilkenhans, T., Siegert, H., and Schlögl, R., *Catal. Today* **32**, 333 (1996).